



# Determination of thermodynamic properties of aluminum based binary and ternary alloys



Yemliha Altıntaş<sup>a</sup>, Sezen Aksöz<sup>b</sup>, Kâzım Keşlioğlu<sup>c,\*</sup>, Necmettin Maraşlı<sup>d</sup>

<sup>a</sup> Abdullah Gül University, Faculty of Engineering, Department of Materials Science and Nanotechnology, 38039, Kayseri, Turkey

<sup>b</sup> Nevşehir Hacı Bektaş Veli University, Faculty of Arts and Science, Department of Physics, 50300, Nevşehir, Turkey

<sup>c</sup> Erciyes University, Faculty of Science, Department of Physics, 38039, Kayseri, Turkey

<sup>d</sup> Yıldız Technical University, Faculty of Chemical and Metallurgical Engineering, Department of Metallurgical and Materials Engineering, 34210, Davutpaşa, İstanbul, Turkey

## ARTICLE INFO

### Article history:

Received 13 May 2015

Received in revised form

30 June 2015

Accepted 6 July 2015

Available online 11 July 2015

### Keywords:

Aluminum alloy

Thermodynamic properties

Interfacial energy

Solidification

Crystal growth

## ABSTRACT

In the present work, the Gibbs–Thomson coefficient, solid–liquid and solid–solid interfacial energies and grain boundary energy of a solid Al solution in the Al–Cu–Si eutectic system were determined from the observed grain boundary groove shapes by measuring the thermal conductivity of the solid and liquid phases and temperature gradient. Some thermodynamic properties such as the enthalpy of fusion, entropy of fusion, the change of specific heat from liquid to solid and the electrical conductivity of solid phases at their melting temperature were also evaluated by using the measured values of relevant data for Al–Cu, Al–Si, Al–Mg, Al–Ni, Al–Ti, Al–Cu–Ag, Al–Cu–Si binary and ternary alloys.

© 2015 Elsevier B.V. All rights reserved.

## 1. Introduction

Aluminum alloys have many advantages that include high thermal and electrical conductivities, low density, high specific strength, ease of casting, high strength to weight ratio and reasonable corrosion resistance. By using appropriate heat treatment techniques [1–6] we can achieve better features. Aluminum alloys have a wide range of applications in the aerospace and automotive industries. In particular, the automotive industry uses aluminum alloys for engine blocks and cylinder heads [6,7].

One of the most important aluminum based alloys is Al–Cu–Si. Because of its low melting temperature and good fluidity, the Al–Cu–Si eutectic alloy has been used in the application of braze welding. Although a lot of research has been carried out on the Al–Cu–Si non-eutectic alloy in the literature [8–10], only a few studies [11] have been done on ternary eutectic Al–Cu–Si alloy systems. From the Al–Cu–Si phase diagram [12], the eutectic composition of Al–Cu–Si alloy is Al-26.82 wt.% Cu-5.27 wt.% Si and the eutectic temperature is 797 K. The eutectic phases of Al-26.82

wt.% Cu-5.27 wt.% Si eutectic alloy are Al solution, Si and  $\theta$ (CuAl<sub>2</sub>). The aim of this study is to evaluate some of the thermo-physical properties of Al-26.82 wt.% Cu-5.27 wt.% Si ternary eutectic alloy such as the Gibbs–Thomson coefficient, solid–liquid interfacial energy, solid–solid interfacial energy, enthalpy of fusion, entropy of fusion, change of specific heats from liquid to solid and the electrical conductivity of solid phases at their melting temperatures.

## 2. Experimental procedure

### 2.1. Sample preparation

The composition of the alloy was chosen as Al-26.82 wt.% Cu-5.27 wt.% Si [12] to grow a single solid Al solution phase on the eutectic casting phase. The Al-26.82 wt.% Cu-5.27 wt.% Si alloy was prepared in a vacuum furnace by using Al, Cu and Si metals with 99.99, 99.9 and 99.999% purities, respectively. The molten alloy was poured into a graphite crucible at the casting furnace and then directionally solidified. The sample was then ready to place in the radial heat flow apparatus.

In order to obtain the grain boundary groove shapes (GBGS) in metallic alloy systems, a radial heat flow apparatus was firstly

\* Corresponding author.

E-mail address: [kesli@erciyes.edu.tr](mailto:kesli@erciyes.edu.tr) (K. Keşlioğlu).

designed by Gündüz and Hunt [13]. The block diagram of the radial heat flow apparatus is shown in Fig. 1. The details of the experimental technique are given in Refs. [13–19]. Similar instruments were used in this study to observe the GBGSs in the Al–Cu–Si.

## 2.2. Microstructure of Al–Cu–Si eutectic system

The microstructure of the alloy was observed through optical microscope and SEM (Scanning Electron Microscope) in different areas of the samples. The specimen was prepared for microscopic observation using standard metallographic techniques. In order to obtain a good image an etchant (2.5 ml nitric acid, 1.5 ml hydrochloric acid, 1 ml hydrofluoric acid in 95 ml water) was used for 15 s. The optical microscope and SEM photographs of the microstructure of the Al–Cu–Si alloy are shown in Fig. 2. The solid phases existed in the Al–Cu–Si systems were clearly shown in Fig. 2c. The photograph of Fig. 2c was taken from cross-sectional area of cylindrical sample which was melted around the central heating element and then annealed a sufficient period in a constant temperature gradient to obtain the GBGS. Fig. 2c has shown the microstructures of solid phases with casting phase away from the solid–liquid interface. According to Fig. 2c the solid  $\alpha$ -Al phase grown on the eutectic structure during the annealing period.

EDX composition analysis was used to determine the three phases of the Al–Cu–Si alloy. The EDX result is illustrated in Fig. 3. As shown in Figs. 2 and 3, the black phase is the Al solid solution, the gray phase is the Si solid solution and the white phase is  $\theta$  ( $\text{CuAl}_2$ ). While the  $\alpha$ -Al and  $\theta$ - $\text{CuAl}_2$  phases grew alongside in accordance with each other, the Si phase disrupted this harmony with its needle like appearance in Fig. 2a, and with its blade like appearance in Fig. 2c. Because the unstable Si phase has a faceted structure, the  $\alpha$ -Al and  $\theta$ - $\text{CuAl}_2$  phases have unafaceted structures.

## 2.3. Determination of Gibbs–Thomson coefficients for solid Al solutions in the Al–Cu–Si eutectic system

In order to determine the Gibbs–Thomson coefficient ( $\Gamma$ ) from

the numerical method firstly constructed by Gündüz and Hunt [13], the groove coordinates of the GBGSs, the thermal conductivity ratio, and the temperature gradient of the solid phase must be known. In the measurement of temperature gradient and groove coordinates the total experimental errors were determined as 6.5% and 0.1%, respectively. Thus the total experimental error in the determination of the Gibbs–Thomson coefficient is about 7%.

### 2.3.1. Determination of Gibbs–Thomson coefficient for solid Al solution in equilibrium with Al–Cu–Si liquid

The GBGS for the Al solid solution in equilibrium with the Al–Cu–Si liquid (Al–26.82 wt.% Cu–5.27 wt.% Si) were observed and a typical GBGS was shown in Fig. 4. To determine the Gibbs–Thomson coefficients ( $\Gamma$ ) for the Al solid solution with the numerical model we used ten equilibrated GBGSs. We determined the Gibbs–Thomson coefficients for both sides of these ten groove shapes. The determined values of  $\Gamma$  for the Al solid solution are given in Table 1. The average value of  $\Gamma$  from Table 1 is found to be  $(2.11 \pm 0.15) \times 10^{-7}$  Km.

### 2.3.2. Determination of Gibbs–Thomson coefficient for solid Al solution in equilibrium with the solid $\text{CuAl}_2$

For the first time, the GBGSs for a solid Al solution in equilibrium with solid  $\text{CuAl}_2$  were also observed in the present study and a typical GBGS is shown in Fig. 5. As can be seen from Fig. 5, the solid  $\text{CuAl}_2$  phase has grown in front of the solid Al phase. To determine the Gibbs–Thomson coefficients for the solid Al solution in equilibrium with the solid  $\text{CuAl}_2$ , we used four GBGSs. The values of  $\Gamma$  for the solid Al solution in equilibrium with the solid  $\text{CuAl}_2$  are given in Table 2. The average value of  $\Gamma$  from Table 2 is found to be  $(2.23 \pm 0.16) \times 10^{-7}$  Km.

## 2.4. Determinations of entropy of fusion per unit volume for solid Al solutions

The entropy change per unit volume for an alloy is given by Refs. [13],

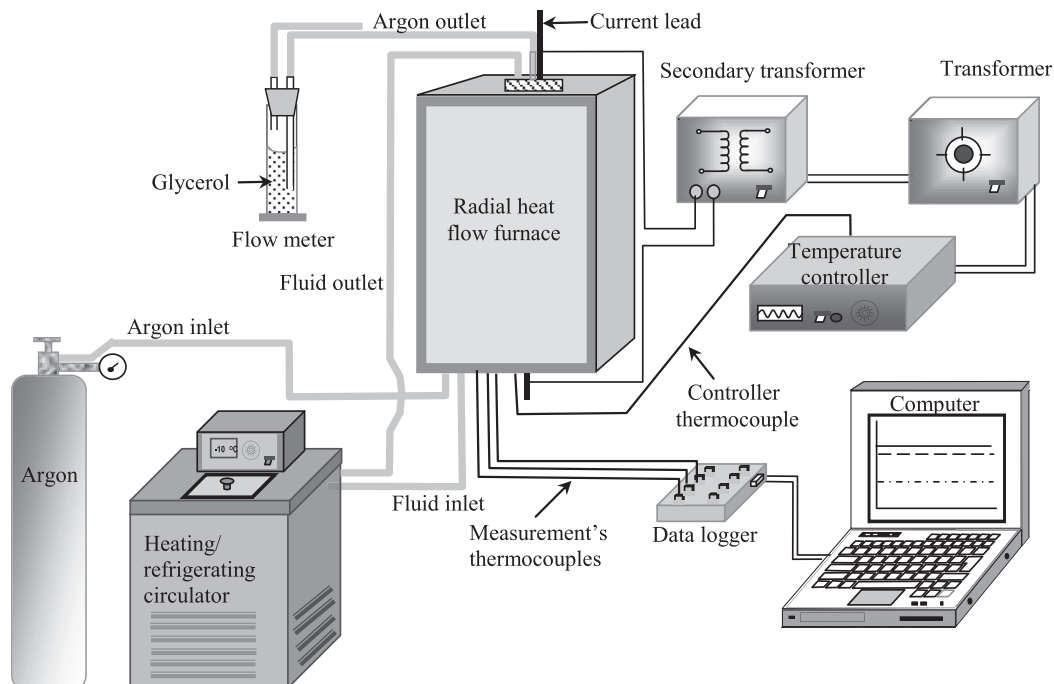
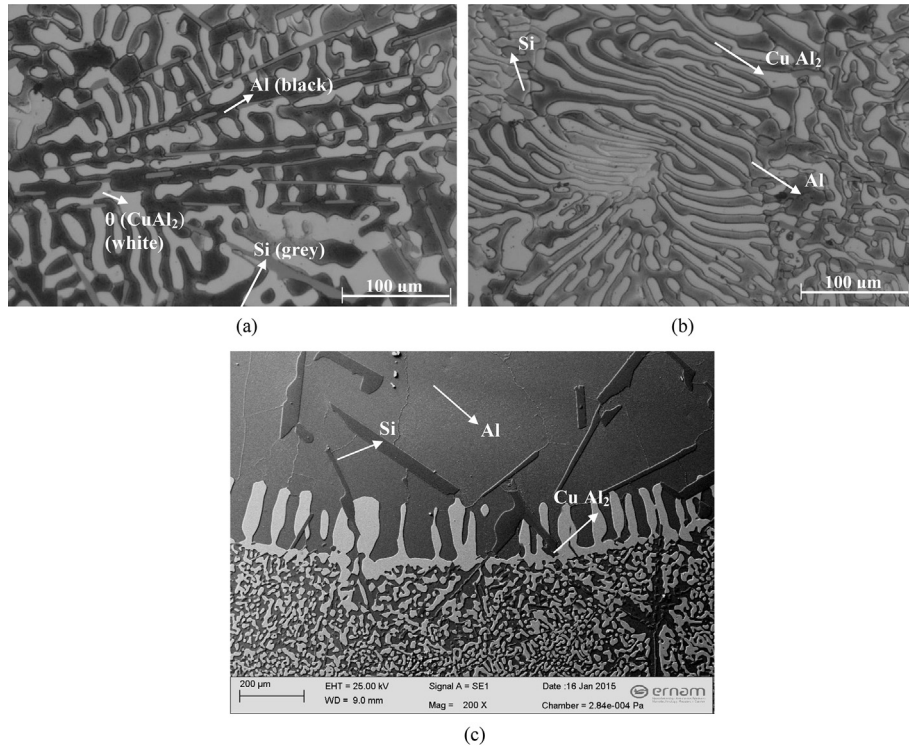
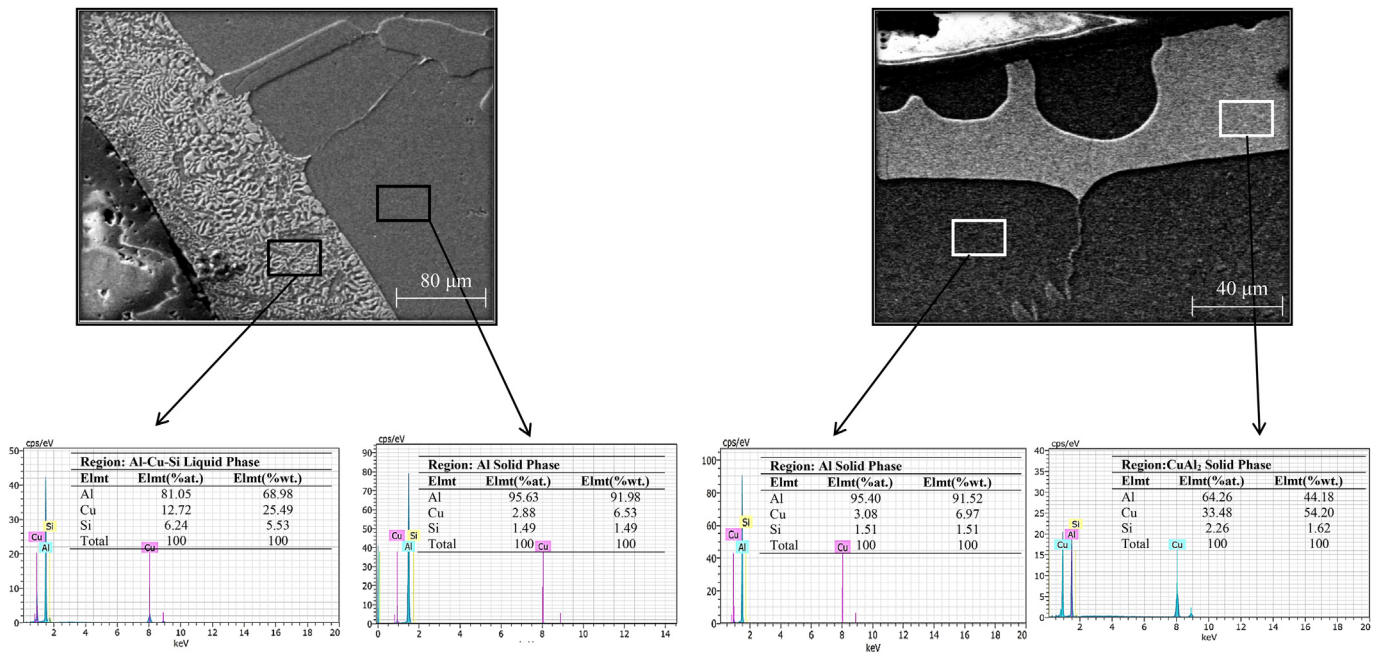


Fig. 1. Block diagram of radial heat flow apparatus.



**Fig. 2.** a) and b) Optical microscope photographs of microstructure of Al-26.82 wt.% Cu-5.27 wt.% Si ternary eutectic alloy from the casting phase, c) SEM photograph of microstructural morphologies of Al-26.82 wt.% Cu-5.27 wt.% Si ternary eutectic alloy.



**Fig. 3.** The chemical composition analysis of the Al–Cu–Si ternary eutectic alloy by using EDX.

$$\Delta S_f = \frac{(1 - C_S)(S_A^L - S_A^S) + C_S(S_B^L - S_B^S)}{V_S} \quad (1)$$

where  $S_A^L$ ,  $S_A^S$ ,  $S_B^L$  and  $S_B^S$  are the partial molar entropies for A and B materials and  $C_S$  is the solid composition. For a sphere [20].

$$\Delta C_L = \frac{2\sigma_{SL}V_S(1 - C_L)C_L}{rRT_M(C_S - C_L)} \quad (2)$$

where  $\Delta C_L$  is the change in liquid composition due to curvature of the interface at constant temperature,  $T_M$  is the melting temperature,  $V_S$  is the molar volume of the solid phase and  $R$  is the gas

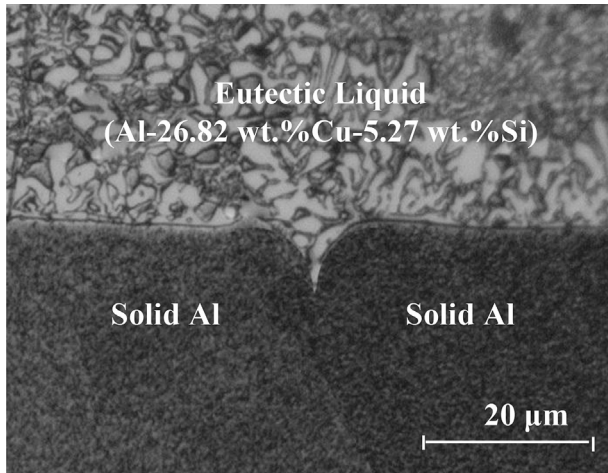


**Fig. 4.** Typical grain boundary groove shape for solid Al solution in equilibrium with the Al-26.82 wt.% Cu-5.27 wt.% Si eutectic liquid.

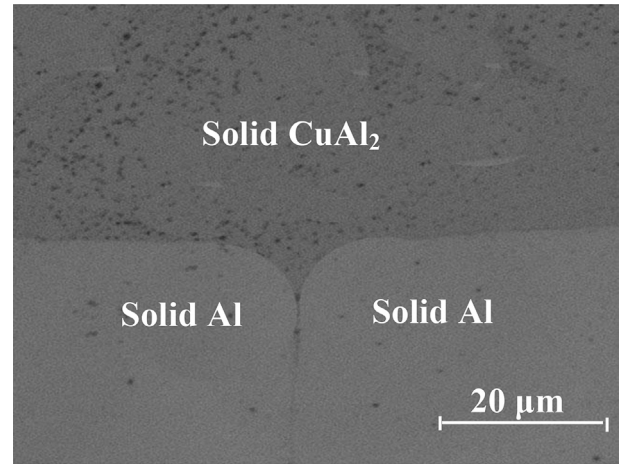


**Fig. 5.** Typical grain boundary groove shape for solid Al solution in equilibrium with the solid CuAl<sub>2</sub> phase.

constant. For small changes

$$\Delta T_r = m_L \Delta C_L = \frac{2 m_L \sigma_{SL} V_S (1 - C_L) C_L}{r R T_M (C_S - C_L)} \quad (3)$$

where  $m_L$  is the liquidus slope. For a spherical solid  $r_1 = r_2 = r$  and the curvature undercooling is written by

$$\Delta T_r = \frac{2 \sigma_{SL}}{r \Delta S_f} \quad (4)$$

From Equations (3) and (4), the entropy change for an alloy is expressed as

$$\Delta S_f = \frac{R T_M}{m_L V_S} \frac{C_S - C_L}{(1 - C_L) C_L} \quad (5)$$

The experimental error in the determination of  $\Delta S_f$  is about 5% [21].

In the present work, it was not possible to determine the value of the entropy of fusion per unit volume for the solid phase in the ternary eutectic system from Eq. (5). For two different temperatures  $T_1$  and  $T_2$  at a constant pressure, the entropy of fusion per unit volume can be expressed as

$$\Delta S_{f1} = \frac{\Delta q_1}{T_1} \quad (6)$$

$$\Delta S_{f2} = \frac{\Delta q_2}{T_2} \quad (7)$$

where  $\Delta q_1$  and  $\Delta q_2$  are the absorbed or emitted heat (enthalpy of fusion or solidification) at the melting temperatures. If the solid phases are the same and the difference between  $T_2$  and  $T_1$  is small, the value of  $\Delta q_1$  should be close to the value of  $\Delta q_2$  i.e.  $\Delta q_1 \approx \Delta q_2$ . Dividing Eq. (6) by Eq. (7) gives

$$\Delta S_{f2} = \Delta S_{f1} \frac{T_1}{T_2} \quad (8)$$

If the value of  $\Delta S_{f1}$  at  $T_1$  is known or determined for a solid phase in the binary eutectic system, the value of  $\Delta S_{f2}$  at  $T_2$  can then be estimated from Eq. (8) by using the values of  $\Delta S_{f1}$ ,  $T_1$  and  $T_2$  for the same solid phase in the ternary eutectic system.

Some physical properties for the solid Al solution in equilibrium with Al-26.82 wt.% Cu-5.27 wt.% Si liquid are given in Table 3. The value of  $\Delta S_f$  for the solid Al solution in the Al<sub>67.91</sub>Cu<sub>26.82</sub>Si<sub>5.27</sub> was determined to be  $0.69 \times 10^6 \text{ J K}^{-1} \text{ m}^{-3}$  from Eq. (8) by using the relevant parameters and is also given in Table 3.

### 2.5. Determination of enthalpy of fusion and specific heat change for solid Al solutions

To determine the enthalpy of fusion we have to know the entropy of fusion per unit volume and it can be expressed as

**Table 1**  
The Gibbs–Thomson coefficients for solid Al solution in equilibrium with the Al-26.82 wt.% Cu-5.27 wt.% Si eutectic liquid. The subscripts LHS and RHS refer to left hand side and right hand side of the groove respectively.

Groove No	$G_K \times 10^2 \text{ (K/m)}$	$\alpha^\circ$	$\beta^\circ$	Gibbs–Thomson coefficient	
				$\Gamma_{\text{LHS}} \times 10^{-7} \text{ (Km)}$	$\Gamma_{\text{RHS}} \times 10^{-7} \text{ (Km)}$
1	17.65	23.4	18.0	2.21	2.02
2	16.74	14.5	14.8	2.06	2.04
3	16.88	24.1	28.2	2.36	2.19
4	16.65	11.5	10.6	2.12	1.97
5	18.29	7.3	9.2	1.98	1.93
6	19.64	5.7	11.2	2.21	1.99
7	17.08	6.8	11.2	2.32	2.01
8	18.36	17.8	16.1	2.10	1.98
9	18.58	17.6	15.9	2.07	2.23
10	19.79	10.3	8.1	2.18	2.14
				$\bar{T} = (2.11 \pm 0.15) \times 10^{-7} \text{ Km}$	

**Table 2**

The Gibbs–Thomson coefficients for solid Al solution in equilibrium with the solid CuAl<sub>2</sub>. The subscripts LHS and RHS refer to left hand side and right hand side of the groove respectively.

Groove No	$G_K \times 10^2$ (K/m)	$\alpha^\circ$	$\beta^\circ$	Gibbs–Thomson coefficient	
				$\Gamma_{LHS} \times 10^{-7}$ (Km)	$\Gamma_{RHS} \times 10^{-7}$ (Km)
1	20.00	23.4	18.0	2.26	2.23
2	20.36	14.5	14.8	2.27	2.23
3	19.75	24.1	28.2	2.09	2.22
4	20.45	11.5	10.6	2.26	2.28
				$\bar{T}=(2.23 \pm 0.16) \times 10^{-7}$ Km	

**Table 3**

Some thermophysical properties for solid Al solution in equilibrium with Al-26.82wt.% Cu-5.27 wt.% Si eutectic liquid.

Alloy	Solid phase	Liquid phase	Eutectic melting Point (K)	$\Delta S_f$ (J K <sup>-1</sup> m <sup>-3</sup> )
Al–Cu [13]	Al-5.7 wt.% Cu	Al-33 wt.% Cu	821	$0.67 \times 10^6$
Al–Cu–Si [12]	Al	Al-26.82 wt.% Cu-5.27 wt.% Si	795	$0.69 \times 10^6$

$$\Delta S_f = \frac{\Delta H_M}{T_M} \frac{1}{V_S} \quad (9)$$

where  $\Delta H_M$  is the enthalpy change of the solid phase at melting temperature and  $T_M$  is the melting temperature.

Enthalpies of fusion ( $\Delta H_M$ ) for solid Al solution phases in the binary or ternary alloys were determined by using the values of the entropy of fusion per unit volume, the melting temperature and the molar volume in Eq. (9).

At constant pressure the specific heat is expressed as

$$C_p = \left( \frac{\partial H}{\partial T} \right)_p \quad (10)$$

Therefore the variation of enthalpy (H) with temperature (T) can be obtained from the knowledge of the variation of specific heat with temperature. A phase change from a low- to a high-temperature phase is always endothermic, and hence the  $\Delta H_M$  for the change is always a positive quantity. Thus  $\Delta H_M$ , the molar latent heat of melting, which is the difference between the enthalpy of a mole of liquid and the enthalpy of a mole of solid, is always positive. The specific heat change can be obtained as follows:

For liquid state,

$$C_{P(liquid)} = \left( \frac{\partial H_{liquid}}{\partial T} \right)_p \quad (11)$$

For solid state,

$$C_{P(solid)} = \left( \frac{\partial H_{solid}}{\partial T} \right)_p \quad (12)$$

Subtracting Eqs. (11) and (12) gives

$$C_{P(liquid)} - C_{P(solid)} = \left( \frac{\partial H_{liquid}}{\partial T} \right)_p - \left( \frac{\partial H_{solid}}{\partial T} \right)_p \quad (13)$$

$$\Delta C_p = \left( \frac{\partial (H_{liquid} - H_{solid})}{\partial T} \right)_p \quad (14)$$

or

$$\Delta C_p = \left( \frac{\partial \Delta H}{\partial T} \right)_p \quad (15)$$

At the melting temperature ( $T_M$ ), the Eq. (15) can be written as

$$\Delta H_m = \Delta C_p T_M \quad (16)$$

The enthalpies of fusion ( $\Delta H_M$ ) for solid Al solution phases in the binary or ternary alloys were calculated from Eq. (9) and then the changes of specific heats ( $\Delta C_p$ ) were determined from Eq. (16) and they are also given in Table 4. The calculated values of  $\Delta C_p$  for the Al solution phase in different binary and ternary systems are close to each other, except the value of  $\Delta C_p$  for the Al solution in the Al–Si binary system. Due to the fact that silicon in Al–Si binary alloy has a faceted microstructure and a high entropy of fusion value, the values of enthalpy of fusion and specific change of heat for Al–Si are higher than the other Al based binary and ternary alloy systems in Table 4.

## 2.6. Evaluation of solid–liquid and solid–solid interfacial energy for solid Al solutions in the Al–Cu–Si eutectic alloy

The solid–liquid interfacial energy ( $\sigma_{SL}$ ) for isotropic condition [13] can be determined as

$$\Gamma = \frac{\sigma_{SL}}{\Delta S_f} \quad (17)$$

In order to obtain  $\sigma_{SL}$  from Eq. (17), one needs to know the values of  $\Gamma$  and  $\Delta S_f$ . The solid–liquid interfacial energy between the solid Al solution and Al-26.82 wt.% Cu-5.27 wt.% Si liquid and the solid–solid interfacial energy of the solid Al solution in equilibrium with solid CuAl<sub>2</sub> were determined to be  $(145.3 \pm 17.4) \times 10^{-3}$  J m<sup>-2</sup> and  $(153.9 \pm 18.3) \times 10^{-3}$  J m<sup>-2</sup>, respectively. The total experimental error of determining the solid–liquid interfacial energy in this study is about 12%.

## 2.7. Calculation of grain boundary energy for solid Al solutions in the Al–Cu–Si eutectic alloy

If the grains are the same on both sides of the groove, the grain boundary energy can be stated by

$$\sigma_{gb} = 2\sigma_{SL} \cos\left(\frac{\theta_A + \theta_B}{2}\right) \quad (18)$$

where  $\theta_A$  and  $\theta_B$  are the angles that both sides of the groove shapes

**Table 4**  
Thermodynamic properties for Al rich alloys at the eutectic melting temperature.

Alloy	Melting temperature $T_M$ (K)	Molar volume of solid Al $V_{Al} \times 10^{-6}$ (m <sup>3</sup> )	Entropy change of fusion $\Delta S_f \times 10^6$ (J/K m <sup>3</sup> )	Enthalpy change of fusion ( $\Delta H$ ) (J/mol)	Change of specific heat ( $\Delta C_p$ ) (J/mol K)
Al-5.7 wt.% Cu	821	9.90	0.67 [13]	5446	6.6
Al-5.7 wt.% Cu	831	9.90	0.67 [14]	5512	6.6
Al-1.67 wt.% Si	850	9.96	0.86 [13]	7281	8.6
Al-42.09 wt.% Ag-7.5 wt.% Cu	775	9.81	0.61 [22]	4638	6.0
Al-26.82 wt.% Si-5.27 wt.% Cu	795	9.90	0.69 [PW]	5431	6.8

make with the y axis. From the Eq. (18),  $\sigma_{gb} \leq 2\sigma_{SL}$ .

The value of the grain boundary energy between the solid Al solution and the Al–Cu–Si liquid and between the solid Al solution and solid  $CuAl_2$  were found to be  $(279.3 \pm 36.3) \times 10^{-3} \text{ J m}^{-2}$  and  $(302.4 \pm 39.3) \times 10^{-3} \text{ J m}^{-2}$ , respectively from Eq. (18). In the evaluation of  $\theta$ , the experimental error is just about 1%. Thus the total experimental error in the calculation of grain boundary energy is about 13%.

The anisotropy of the interfacial energy is crucial for phase transformations. However the exact determination of this value is very difficult and there are a limited number of studies in the literature. Since the anisotropy of interfacial energy for solid Al solution is unknown, the interfacial energy between the Al solid solution and Al–Cu–Si liquid was supposed to be isotropic in this study.

The values of  $\Gamma$ ,  $\sigma_{SL}$  and  $\sigma_{gb}$  for the solid Al solution determined in this study were compared with the similar quantities for Al based binary and ternary alloys evaluated in previous works. The comparison of these values and their good agreement in the limits of experimental errors can be seen in Table 5. The values obtained by Bulla et al. [24] disagree with the other works in Table 5. In Ref. [24] the value of  $\Gamma$  for Al solution was found to be in the range of  $4.4 \times 10^{-8}$ – $8.1 \times 10^{-8}$  km. The average value of  $\Gamma$  obtained by Ref. [24] is three times smaller than the value of  $\Gamma$  obtained in the present and previous works. Thus the value of solid–liquid interfacial energy obtained by Ref. [24] is lower than the other values of solid–liquid interfacial energies in Table 5.

## 2.8. Determination of electrical conductivity for solid Al solutions

Investigations of the thermal and electrical properties of aluminum rich alloys are important for many technological applications. Thermal and electrical conductivity play a crucial role in testing the performance and stability of alloys. In the literature, there is not much information about the thermal and electrical properties of Al rich alloys. Thus, determining the thermal and electrical properties for Al rich alloys could be of great use to

researchers and engineers. The determination of thermal and electrical conductivity values were achieved in two steps. Firstly the variations in the thermal conductivity of the solid phases with temperature were measured for different compositions of Al rich alloys. Secondly the variations in electrical conductivity with temperature were calculated via the Wiedemann–Franz law and Smith–Palmer equation for the same materials.

The thermal conductivity of solid Al phase has measured by using the radial heat flow apparatus and the details of procedure can be learn in Refs. [13–17]. To measure the thermal conductivity, the inside of the cylindrical specimen was heated with a heating wire and the outside of the sample was cooled by a circulating bath. The temperature gradient of the solid phase in the sample can be calculated by Fourier's law,

$$G_S = \left( \frac{dT}{dr} \right)_S = -\frac{Q}{AK_S} \quad (19)$$

where  $K_S$  is the thermal conductivity of solid phase,  $Q$  is the power on the sample,  $A$  is the surface area. When we integrate Eq. (19), it gives Eq. (20).

$$K_S = a_0 \frac{Q}{T_1 - T_2} \quad (20)$$

where  $a_0 = \ln(r_2/r_1)/2\pi\ell$  is an experimental constant,  $\ell$  is the length of the heating wire,  $T_1$  and  $T_2$  are the temperatures of the thermocouples,  $r_1$  and  $r_2$  are the distances from the center of the sample. The reliable thermal conductivity values can be determined by measuring the  $Q$ ,  $r_1$ ,  $r_2$ ,  $\ell$ ,  $T_1$  and  $T_2$  values.

Since both the electrical and heat transportation of the metal depend on free electrons, the ratio of thermal conductivity ( $K$ ) to electrical conductivity ( $\sigma$ ) is proportional to the temperature of the metal. This fact is discovered by the Wiedemann–Franz law,

**Table 5**  
A comparison of the values of  $\Gamma$ ,  $\sigma_{SL}$  and  $\sigma_{gb}$  for solid Al solution obtained in the present work with the values of  $\Gamma$ ,  $\sigma_{SL}$  and  $\sigma_{gb}$  obtained in previous works for similar binary and ternary alloys.

System	Solid phase	Liquid phase	Temperature (K)	Entropy $\Delta S_f \times 10^6$ (J/K m <sup>3</sup> )	$\Gamma \times 10^{-7}$ (Km)	$\sigma_{SL} \times 10^{-3}$ (J m <sup>-2</sup> )	$\sigma_{gb} \times 10^{-3}$ (J m <sup>-2</sup> )
Al–Cu	Al (Al-2.5 at% Cu)	Al-17.3 at% Cu	821	0.67 [13]	2.41 ± 0.19 [13]	163.40 ± 21.24 [13]	324.70 ± 45.46 [13]
Al–Si	Al (Al-1.59 at% Si)	Al-12.1 at% Si	850	0.86 [13]	1.96 ± 0.16 [13]	168.95 ± 21.96 [13]	336.50 ± 47.11 [13]
Al–Mg	Al (Al-18.9 at% Mg)	Al-37.4 at% Mg	723	1.15 [25]	1.30 ± 0.10 [25]	149.20 ± 19.40 [25]	295 ± 41 [25]
Al–CuAl <sub>2</sub>	Al (Al-2.5 at% Cu)	Al-17.3 at% Cu	831	0.67 [14]	2.36 ± 0.16 [14]	160.01 ± 19.20 [14]	–
Al–NiAl <sub>3</sub>	Al (Al-0.023 at%Ni)	Al-3.06 at%Ni	913	0.92 [14]	1.86 ± 0.13 [14]	171.56 ± 20.58 [14]	336.50 ± 47.11 [14]
Al–Ti	Al (Al-0.186 at% Ti)	Al-0.0169 at% Ti	938	1.33 [14]	1.31 ± 0.09 [14]	174.62 ± 20.95 [14]	335.14 ± 46.92 [14]
Al–Ti	Al (Al-0.186 at% Ti)	Al-0.0169 at% Ti	938	1.33 [23]	1.28 ± 0.06 [23]	170.72 ± 16.22 [23]	332.01 ± 35.19 [23]
Al–Cu–Ag	Al (Al-16.42 at% Ag-4.97 at% Cu)	Al-16.57 at% Ag-11.87 at% Cu	775	1.07 [24]	0.63 ± 0.14 [24]	67 ± 15 [24]	–
Al–Cu–Ag	Al (Al-16.42 at% Ag-4.97 at% Cu)	Al-16.57 at% Ag-11.87 at% Cu	775	0.61 [22]	2.29 ± 0.16 [22]	137.40 ± 16.49 [22]	268.20 ± 34.87 [22]
Al–Cu–Si	Al (Al-2.88 at% Cu-1.49 at% Si)	Al-13.5 at% Cu-6 at% Si	795	0.69 [PW]	2.11 ± 0.15 [PW]	145.30 ± 17.40 [PW]	279.30 ± 36.30 [PW]

PW: Present Work.

**Table 6**

Thermal and electrical conductivities for some Al rich alloys at the eutectic melting temperature.

Alloy	Melting temperature $T_M$ (K)	Thermal conductivity K (W/Km)	Electrical conductivity (Smith–Palmer) $\sigma \times 10^8$ (1/ $\Omega$ m)	Electrical conductivity (Wiedemann–Franz) $\sigma \times 10^8$ (1/ $\Omega$ m)	Electrical conductivity (experimental) $\sigma \times 10^8$ (1/ $\Omega$ m)
Al-5.7 wt.% Cu	821	135.90 [13]	0.0686	0.0676	–
Al-5 wt.% Cu	835	–	–	–	0.1027 [28]
Al-35 wt.% Cu	821	–	–	–	0.0649 [28]
Al-1.67 wt.% Si	850	108.60 [13]	0.0518	0.0521	–
Al-17.4 wt.% Mg	723	120 [25]	0.0680	0.0677	–
Al-10 wt.% Mg	723	–	–	–	0.0720 [28]
Al-6.4 wt.% Ni	913	76.15 [14]	0.0323	0.0340	–
Al-0.22 wt.% Ti	938	129.70 [14]	0.0571	0.0564	–
Al-42.09 wt.% Ag-7.5 wt.% Cu	775	152.99 [24]	0.0825	0.0806	–
Al-42.09 wt.% Ag-7.5 wt.% Cu	775	140.92 [22]	0.0756	0.0742	–
Al-6 wt.% Si-3 wt.% Cu	811	–	–	–	0.0747 [27]

$$\frac{K}{\sigma} = LT \quad (21)$$

where T is the temperature and L is the Lorenz number and it is equal to

$$L = \frac{\pi^2}{3} \left( \frac{k_B}{e} \right)^2 = 2.44 \times 10^{-8} W\Omega K^{-2} \quad (22)$$

A modified form of the Lorenz equation, known as the Smith–Palmer equation, can be used to estimate the thermal conductivity [26]. In particular, the Smith–Palmer equation for aluminum alloys (without silicon) can be written as

$$K = 0.909L\sigma T + 10.5 \quad (23)$$

The values of thermal conductivity for Al–Cu [13], Al–Si [13], Al–Mg [22], Al–Ni [14], Al–Ti [14], Al–Cu–Ag [24,25], Al–Cu–Si [27] alloys at their melting temperatures were taken from the literature. Then the electrical conductivity values for these aluminum based binary and ternary alloys at their melting temperatures were calculated from the Wiedemann–Franz law and Smith–Palmer equation separately by using K and L values; the values are given in Table 6.

As can be seen from Table 6, the electrical conductivity values obtained from the Smith–Palmer equation and the Wiedemann–Franz law are compatible with each other. Also, the calculated values of electrical conductivity for Al rich alloys agree well with the values of electrical conductivity experimentally measured in previous works [27,28] for Al rich binary and ternary alloys.

### 3. Conclusions

Some of the thermophysical properties and the microstructure of aluminum based binary or ternary alloys were investigated. The results obtained in this work can be summarized as follows:

- The microstructure of the Al-26.82 wt.% Cu-5.27 wt.% Si alloy was observed through SEM (Scanning Electron Microscope) in different areas of the samples. The three eutectic phases ( $\alpha$ -Al, Si, CuAl<sub>2</sub>) of the Al–Cu–Si alloy were strictly determined by EDX analysis.
- The GBGSs between the solid Al solution and the Al–Cu–Si liquid and between the solid Al solution and the solid CuAl<sub>2</sub> solution were viewed. The Gibbs–Thomson coefficients, solid–liquid interfacial energy, solid–solid interfacial energy and grain boundary energies between the solid Al solution and the Al–Cu–Si liquid and between the solid Al solution and solid CuAl<sub>2</sub> solution were determined. When we compare the

determined values for the Al–Cu–Si system with similar previous works, we find very good compatibility.

- The entropy of fusion ( $\Delta S_f$ ), enthalpy of fusion ( $\Delta H_M$ ) and the change of specific heat ( $\Delta C_p$ ) for solid Al solutions in the binary and ternary alloys were determined by using the measured relevant physical properties of the solid Al solution phases.
- The electrical conductivities for the solid Al solution phases at their melting temperatures were calculated from the Wiedemann–Franz law and Smith–Palmer equation by using the measured values of K and L. The calculated electrical conductivity values are compatible with each other and with experimentally measured previous works.

### Acknowledgments

This project was supported by Erciyes University Scientific Research Project Unit under Contract No: FDK-2013-4467. The authors would like to thank Erciyes University's Scientific Research Project Unit for their financial support. Yemilha Altıntas would like to thank TUBITAK for their support through a scholarship.

### References

- W.R. Osorio, D.J. Moutinho, L.C. Peixoto, I.L. Ferreira, A. Garcia, Macro segregation and microstructure dendritic array affecting the electrochemical behavior of ternary Al–Cu–Si alloys, *Electrochimica Acta* 56 (2011) 8412–8421.
- G.A. Capuano, W.G. Davenport, Electrodeposition of aluminum from alkyl benzene electrolytes, *J. Electrochem. Soc.* 118 (1971) 1688–1695.
- M. Azarbarmas, M. Emamy, J.R. Deh, M. Alipour, M. Karamouz, The effects of Be on mechanical properties of Al–Mg<sub>2</sub>Si in situ composite, the minerals, metals and materials society, in: Supplemental Proceedings: General Paper Selections, 3, John Wiley & Sons, Inc, Hoboken, NJ, USA, 2011, <http://dx.doi.org/10.1002/9781118062173.ch109>.
- V.V. Krisyuk, L. Aloui, N.P. Home, B. Saraprata, F. Senocq, D. Samelior, C. Vahlas, CVD of pure copper films from a novel Amidinate Precursor, *Electrochem. Soc.* 25 (2009) 581–586.
- G. García-García, J. Espinoza-Cuadra, H. Mancha-Molinar, Copper content and cooling rate effects over second phase particles behavior in industrial aluminum–silicon alloy 319, *Mater. Des.* 28 (2007) 428–433.
- A.M. Samuel, F.H. Samuel, H.W. Doty, Observations on the formation of  $\beta$ -Al<sub>5</sub>FeSi phase in 319 type Al–Si alloys, *J. Mater. Sci.* 31 (1996) 5529–5539.
- I. Guillot, B. Barlas, G. Cailletaud, M. Clavel, D. Massinon, Thermomechanical fatigue and aging cast aluminium alloy: a link between numerical modeling and microstructural approach, *Int. Conf. Temperature-Fatigue Interact.* 29 (2002) 75–84.
- D.O. Ovono, I. Guillot, D. Massinon, The microstructure and precipitation kinetics of a cast aluminium alloy, *Scr. Mater.* 55 (2006) 259–262.
- M. Legros, B. Kaouache, P. Gergaud, O. Thomas, G. Dehm, T.J. Balk, E. Arzt, Pipe-diffusion ripening of Si precipitates in Al-0.5%Cu-1%Si thin films, *Phil. Mag.* 85 (2005) 3541–3552.
- M.E. Thomas, T.K. Keyser, E.K.W. Goo, Interfacial CuAl<sub>2</sub> precipitate nucleation and growth during the deposition of Al-4%Cu-1.5%Si alloys, *J. Appl. Phys.* 59 (1986) 3768–3773.
- R. Ying, W. BingBo, Rapid solidification of undercooled Al–Cu–Si eutectic alloys, *Chin. Sci. Bull.* 54 (2009) 53–58.
- N. Ponweiser, K.W. Richter, New investigation of phase equilibria in the

- system Al–Cu–Si, *J. Alloys Compd.* 512 (2012) 252–263.
- [13] M. Gündüz, J.D. Hunt, The measurement of solid–liquid surface energies in the Al–Cu, Al–Si and Pb–Sn systems, *Acta Metall.* 33 (1985) 1651–1672.
- [14] N. Maraşlı, J.D. Hunt, Solid–liquid surface energies in the Al–CuAl<sub>2</sub>, Al–NiAl<sub>3</sub> and Al–Ti systems, *Acta Mater* 44 (1996) 1085–1096.
- [15] K. Keşlioğlu, N. Maraşlı, Solid-liquid interfacial energy of the eutectoid beta phase in the Al–Zn eutectic system, *Mater. Sci. Eng. A* 369 (2004) 294–301.
- [16] Y. Ocak, S. Akbulut, K. Keşlioğlu, N. Maraşlı, Solid-liquid interfacial energy of neopentylglycol, *J. Colloid Interface Sci.* 320 (2008) 555–562.
- [17] M. Erol, K. Keşlioğlu, N. Maraşlı, Solid-liquid interfacial energy of the solid Mg<sub>2</sub>Zn<sub>11</sub> phase in equilibrium with Zn–Mg eutectic liquid, *J. Physics-Condensed Matter* 19 (2007) 176003.
- [18] S.B. Karadağ, Y. Altıntaş, E. Öztürk, S. Aksöz, K. Keşlioğlu, N. Maraşlı, Solid–liquid interfacial energy of solid succinonitrile solution in equilibrium with succinonitrile–neopentylglycol eutectic liquid, *J. Cryst. Growth* 380 (2013) 209–217.
- [19] Y. Altıntaş, E. Öztürk, S. Aksöz, K. Keşlioğlu, N. Maraşlı, The experimental determination of interfacial energies for solid Sn in equilibrium with Sn–Mg–Zn liquid, *Metals Mater. Int.* 21 (2015) 286–294.
- [20] J.W. Christian, *The Theory of Transformations in Metals and Alloys, Part I, second ed.*, 1975. Oxford, Pergamon.
- [21] M. Tassa, J.D. Hunt, The measurement of Al–Cu dendrite tip and eutectic interface temperatures and their use for predicting the extent of the eutectic range, *J. Cryst. Growth* 34 (1976) 38–48.
- [22] K. Keşlioğlu, Y. Ocak, S. Aksöz, N. Maraşlı, E. Çadırılı, H. Kaya, Determination of interfacial energies for solid Al solution in equilibrium with Al–Cu–Ag liquid, *Met. Mater. Int.* 16 (2010) 51–59.
- [23] K. Keşlioğlu, M. Gündüz, H. Kaya, E. Çadırılı, Solid-liquid interfacial energy in the Al–Ti system, *Mater. Lett.* 58 (2004) 3067.
- [24] A. Bulla, C. Carreno-Bodensiek, B. Pustal, R. Berger, A. Bührig-Polaczek, A. Ludwig, Determination of the solid-liquid interface energy in the Al–Cu–Ag system, *Metall. Mater. Trans. A* 38 (2007) 1956–1963.
- [25] M. Gündüz, J.D. Hunt, Solid-liquid surface-energy in the Al–Mg system, *Acta Metall.* 37 (1989) 1839–1845.
- [26] D.R. Poirier, G.H. Geiger, *Transport Phenomena in Materials Processing, Mineral, Metals and Materials Society, Warrendale, PA, 1994, pp. 196–198.*
- [27] R. Brandt, G. Neuer, Electrical resistivity and thermal conductivity of pure aluminum and aluminum alloys up to and above the melting temperature, *Int. J. Thermophys.* 28 (2007) 1429–1446.
- [28] C.Y. Ho, M.W. Ackerman, K.Y. Wu, T.N. Havil, R.H. Bogaard, R.A. Matula, S.G. Oh, H.M. James, Electrical resistivity of ten selected binary alloy systems, *J. Phys. Chem. Ref. Data* 12 (1983) 183–319.